Eur. Phys. J. D (2014) 68: 225
DOI: 10.1140/epjd/e2014-40687-4

THE EUROPEAN PHYSICAL JOURNAL D

Regular Article

Mapping the two-component atomic Fermi gas to the nuclear shell-model

Cem Özen[1,2] and Nikolaj Thomas Zinner[3,4,a]

[1] Center for Theoretical Physics, Sloane Physics Laboratory, Yale University, New Haven, CT 06520, USA
[2] Faculty of Engineering and Natural Sciences, Kadir Has University, 34083 Istanbul, Turkey
[3] Department of Physics, Harvard University, Cambridge, MA 02138, USA
[4] Department of Physics and Astronomy, Aarhus University, 8000 Aarhus C, Denmark

Received 2 November 2013 / Received in final form 30 April 2014
Published online 12 August 2014 –

Abstract. The physics of a two-component cold Fermi gas is now frequently addressed in laboratories. Usually this is done for large samples of tens to hundreds of thousands of particles. However, it is now possible to produce few-body systems (1–100 particles) in very tight traps where the shell structure of the external potential becomes important. A system of two-species fermionic cold atoms with an attractive zero-range interaction is analogous to a simple model of nucleus in which neutrons and protons interact only through a residual pairing interaction. In this article, we discuss how the problem of a two-component atomic Fermi gas in a tight external trap can be mapped to the nuclear shell-model so that readily available many-body techniques in nuclear physics, such as the Shell-Model Monte Carlo (SMMC) method, can be directly applied to the study of these systems. We demonstrate an application of the SMMC method by estimating the pairing correlations in a small two-component Fermi system with moderate-to-strong short-range two-body interactions in a three-dimensional harmonic external trapping potential.

1 Introduction

The physics of ultracold gases has seen a rapid development over the past decade [1–3]. An interesting goal in the boundary of few- and many-body systems is the implementation of optical microtraps that can hold a small number of particles. This was recently achieved by the Jochim group in Heidelberg [4,5]. These experiments were performed in a regime where the trapping shell structure became prominent. In theoretical investigations of these systems, large quantum fluctuations would invalidate the use of mean-field approaches such as the BCS method due to the small number of particles involved; hence, many-body approaches beyond the mean-field are needed. Also, the problem of a small number of fermions interacting with each other in the presence of external fields – which provide a level structure – is very similar to the nuclear pairing problem which was initially described in the seminal work of Bohr et al. [6]. There is thus a strong incentive to transfer methods from nuclear physics into cold atomic gases [7,8].

In this article we outline the mapping of a two-component atomic Fermi gas, confined by a tight external trap and interacting through a zero-range interaction, onto the nuclear shell-model in detail. For the benefit of both nuclear and atomic physics communities, the explicit evaluation of the matrix elements of the zero-range interaction in the nuclear shell-model is given in considerable detail in the Appendix. We then investigate the pairing correlations of small systems (less than 20 particles) using the Shell-Model Monte Carlo (SMMC) technique that has been succesful in nuclear physics [9–11]. Also we briefly comment on some of the similarities and differences in studies of the pairing phenomena in the fields of atomic and nuclear physics. Our discussion of the pairing correlations through a two-body BCS-like pairing matrix, to the best of our knowledge, has not been considered in the context of small ultracold Fermi systems in traps before.

A number of different approaches have been used in recent years to address the energetics, structure, and other properties of small Fermi systems [7,12–15]. Although we will briefly comment on and relate to these developments as we proceed, the purpose of this study is not to make a detailed quantitative comparison of various methods in use. Instead, we describe the technical issue of mapping the atomic gas problem in order to apply the SMMC method, a traditional nuclear physics tool, in studies of small ultracold Fermi systems. On a side note, the mapping could also provide a natural connection between atomic and nuclear physics given the prospect that ultracold atomic systems with spin-orbital momentum coupling – a central tenet in nuclear shell-model – may soon be realized.

[a] e-mail: zinner@phys.au.dk

2 Mapping the Fermi gas to the nuclear shell-model

The two-component ultracold fermionic atomic gas consists of neutral atoms, usually alkali species, that occupy two different internal states. The actual internal states are hyperfine states of different projection that can be split by a magnetic field [3]. The energy scale of the hyperfine splitting is by far larger than any other energy scale in the problem so that no internal process in the gas can transfer atoms between the hyperfine levels; thus, one may think of these levels as frozen degrees of freedom. Also, since these systems are usually dilute, the range of the atom-atom interactions is very short compared to the typical interparticle distance. Therefore, the simple zero-range potential is a popular and highly successful model.

The three-dimensional N-body Fermi system in an isotropic harmonic trap with a zero-range interaction of strength V_0 can be described by the Hamiltonian

$$H = \sum_i \frac{\vec{p}_i^2}{2m} + \sum_i \frac{1}{2} m\omega^2 \vec{r}_i^2 + \sum_{[ij]} V_0 \delta(\vec{r}_i - \vec{r}_j), \qquad (1)$$

where i, j denote the particles, $[ij]$ denotes the sum over all pairs of particles, m is the mass of the particles, and ω is the external trapping angular frequency. The oscillator length which we will use later is given by $b = \sqrt{\hbar/m\omega}$. We note that the isotropic three-dimensional oscillator potential has shell closures at $N = 2$, 8, and 20 (the s, $s+p$, and $s + p + sd$ shell configurations in typical nuclear physics language). These will be prominent features in our examples later. In the following, we use the notation where the matrix elements of a general two-body interaction V_{int} are given by

$$\langle \psi_a(\vec{r}_1)\psi_b(\vec{r}_2)|V_{int}|\psi_c(\vec{r}_1)\psi_d(\vec{r}_2)\rangle, \qquad (2)$$

in which the two-body wave functions $\psi_a(\vec{r}_1)\psi_b(\vec{r}_2)$ and $\psi_c(\vec{r}_1)\psi_d(\vec{r}_2)$ must be antisymmetric under the exchange of coordinates.

In a tight harmonic trap (small trapping length, $b = \sqrt{\frac{\hbar}{m\omega}}$), the quantum numbers of single-particle levels are given by n, l, m_l. The two internal hyperfine states can now be mapped onto the spin of a single species of nucleon $m_s = \pm 1/2$. Thus, any single-particle state is uniquely described by $a = (n_a l_a m_{l_a} m_{s_a})$. Any two-body state constructed from these states will have an external and an internal part that combine to determine the overall symmetry. We use a zero-range interaction and the spatial part must thus be non-zero at the origin to give a contribution. This is only possible with a relative wave function that is symmetric under particle exchange. Since the particles are fermions, the internal (hyperfine, or pseudospin) state must be antisymmetric, or in the spin 1/2 language, a spin-singlet state. This completes our mapping of the two-component Fermi system in a trap onto the nuclear shell-model with one species of nucleon (proton or neutron). The nuclear mean-field is replaced by the harmonic oscillator and the internal spin states of the nucleon now correspond to the hyperfine states for the atoms.

In general, the three-dimensional zero-range interaction is ill-defined unless properly regularized. As it has been shown by Busch et al. [16], the case of two fermions with different internal states in a harmonic potential interacting via a zero-range interaction cannot only be properly regularized, but in fact has a tractable solution. This solution has been subsequently studied and confirmed by atomic physics experiments [17–20]. In relation to shell-model applications, the issue is always that a finite model space is used. However, having access to the exact solution in the full space of Busch et al. is an excellent starting point for doing many-body problems in both nuclear and atomic physics [21–31]. In the case of the SMMC method that we are concerned with here, the question of regularization was discussed in detail in reference [32].

Below we will be using strengths $g = -V_0/(\hbar\omega b^3) = 10$ and $g = 20$. The strength can also be given in terms of the two-body scattering length, a. For $g = 10$ we have $a/b = -1.0$ and for $g = 20$ we have $a/b = 11$. Comparing to the standard usage in BCS-BEC crossover studies [1,2] the first value $a/b = -1.0$ is on the (deep) BCS side, while the $a/b = 11$ value is on the BEC side but close to the resonance ($a \to \infty$) and thus close to the unitarity limit.

3 Shell-model Monte Carlo method

Quantum Monte Carlo methods have been extensively used in the study of strongly interacting many-body problems (see f.x. Ref. [7] and references therein). An example is the Auxiliary-field Monte Carlo (AFMC) approach of Zhang and collaborators [33–35]. The AFMC method has been used to calculate zero- and finite-temperature properties of the unitary Fermi gas on a lattice [36,37]. As an alternative to the lattice representation, the AFMC is also formulated within the configuration-interaction nuclear shell-model. This approach is known as the Shell-Model Monte Carlo (SMMC) method and has been widely employed in nuclear physics [9–11] and more recently in the study of trapped cold atoms [32,38,39]. The SMMC approach is based on a linearization of the two-body part of the Hamiltonian using the Hubbard-Stratonovich transformation [40,41]. Here we adopt a formulation of this transformation starting from a general Hamiltonian, which can be written in a manifestly time-reversal invariant form:

$$H = \sum_\alpha \left(\epsilon_\alpha \mathcal{O}_\alpha + \epsilon_\alpha^* \bar{\mathcal{O}}_\alpha\right) + \frac{1}{2}\sum_\alpha V_\alpha \left\{\mathcal{O}_\alpha, \bar{\mathcal{O}}_\alpha\right\}, \qquad (3)$$

where O_α are one-body operators in a convenient basis and the V_α are real numbers. The bars denote time-reversed operators. The SMMC approach relies on the Hubbard-Stratonovich (HS) transformation to linearize the many-body evolution operator $e^{-\beta H}$, where β^{-1} may be interpreted as the temperature in the (grand) canonical ensemble. We first divide β into N_t time slices so that

we can express individual terms at different time slices in $e^{-\beta H} = \left[e^{-\Delta\beta H}\right]^{N_t}$ as:

$$e^{-\Delta\beta H} \approx e^{-\Delta\beta\sum_\alpha\left(\epsilon_\alpha\mathcal{O}_\alpha+\epsilon^*_\alpha\bar{\mathcal{O}}_\alpha\right)} \times\prod_\alpha e^{-\Delta\beta\frac{V_\alpha}{4}\left[(\mathcal{O}_\alpha+\bar{\mathcal{O}}_\alpha)^2-(\mathcal{O}_\alpha-\bar{\mathcal{O}}_\alpha)^2\right]}+\mathcal{O}(\Delta\beta)^2,$$

where we used $2\left\{\mathcal{O}_\alpha,\bar{\mathcal{O}}_\alpha\right\} = (\mathcal{O}_\alpha+\bar{\mathcal{O}}_\alpha)^2-(\mathcal{O}_\alpha-\bar{\mathcal{O}}_\alpha)^2$. Quadratic interaction terms can be effectively linearized through the Gaussian integral identity

$$\begin{aligned} e^{-\Delta\beta\frac{V_\alpha}{4}\left[(\mathcal{O}_\alpha+\bar{\mathcal{O}}_\alpha)^2-(\mathcal{O}_\alpha-\bar{\mathcal{O}}_\alpha)^2\right]} &= \frac{\Delta\beta|V_\alpha|}{4\pi} \\ &\times\int d\sigma^R_\alpha d\sigma^I_\alpha e^{-\Delta\beta\frac{|V_\alpha|}{4}\left[\left(\sigma^R_\alpha\right)^2+\left(\sigma^I_\alpha\right)^2\right]} \\ &\times e^{-\Delta\beta\frac{V_\alpha}{2}\left[s_\alpha\sigma^R_\alpha\left(\mathcal{O}_\alpha+\bar{\mathcal{O}}_\alpha\right)+is_\alpha\sigma^I_\alpha\left(\mathcal{O}_\alpha-\bar{\mathcal{O}}_\alpha\right)\right]}, \end{aligned} \quad (4)$$

where the integration variables σ^R_α and σ^I_α are the real auxiliary fields that give the method its name. The sign factors are $s_\alpha = \pm1$ for $V_\alpha < 0$ and $s_\alpha = \pm i$ for $V_\alpha > 0$. Introducing complex fields for each time slice $\sigma_\alpha(\tau_n) = \sigma^R_\alpha(\tau_n)+i\sigma^I_\alpha(\tau_n)$, we arrive at the Hubbard-Stratonovich representation of the many-body evolution operator

$$e^{-\beta H} = \int\mathcal{D}[\sigma]G(\sigma)U_\sigma(\beta,0). \quad (5)$$

Above,

$$\mathcal{D}[\sigma] = \prod_{\alpha,n}\frac{d\sigma_\alpha(\tau_n)d\sigma^*_\alpha(\tau_n)}{2i}\frac{\Delta\beta|V_\alpha|}{4\pi} \quad (6)$$

is the measure of the integral. $G(\sigma)$ is a Gaussian weight

$$G(\sigma) = e^{-\frac{\Delta\beta}{4}\sum_\alpha|V_\alpha||\sigma_\alpha(\tau_n)|^2}. \quad (7)$$

The many-body propagator, $e^{-\beta H}$, is now effectively reduced to a superposition of one-body propagators

$$U_\sigma(\beta,0) = e^{-\Delta\beta h_\sigma(\tau_{N_t})}\ldots e^{-\Delta\beta h_\sigma(\tau_1)}, \quad (8)$$

where the linearized Hamiltonian as a function of the time-dependent auxiliary fields is given by:

$$\begin{aligned} h_\sigma(\tau) = &\sum_\alpha\left(\epsilon_\alpha+\frac{1}{2}s_\alpha V_\alpha\sigma_\alpha(\tau)\right)\mathcal{O}_\alpha \\ &+\left(\epsilon^*_\alpha+\frac{1}{2}s_\alpha V_\alpha\sigma^*_\alpha(\tau)\right)\bar{\mathcal{O}}_\alpha. \end{aligned} \quad (9)$$

In the SMMC, expectation value of an observable Ω at temperature $T = 1/\beta$ is calculated by expressing both the numerator and the denominator of $\langle\Omega\rangle = \mathrm{Tr}_N[\Omega e^{-\beta H}]/\mathrm{Tr}_N e^{-\beta H}$ (where Tr_N denotes a canonical trace for N-particle system) in the HS representation. In order to perform a Monte Carlo integration, a positive definite weight function is defined as

$$W(\sigma) = G(\sigma)|\mathrm{Tr}_N U_\sigma(\beta,0)|.$$

Thus, one can express the thermal expectation values by:

$$\langle\Omega\rangle = \frac{\int\mathcal{D}[\sigma]W(\sigma)\Phi(\sigma)\langle\Omega\rangle_\sigma}{\int\mathcal{D}[\sigma]W(\sigma)\Phi(\sigma)}, \quad (10)$$

where $\Phi(\sigma) = \mathrm{Tr}_N U_\sigma(\beta,0)/|\mathrm{Tr}_N U_\sigma(\beta,0)|$ is the "sign" and $\langle\Omega\rangle_\sigma = \mathrm{Tr}_N|\Omega U_\sigma(\beta,0)|/\mathrm{Tr}_N U_\sigma(\beta,0)$. The observable $\langle\Omega\rangle$ is then computed in a Monte Carlo integration by selecting an ensemble of auxiliary fields $(\sigma_1,\ldots,\sigma_N)$ sampled according to the distribution function $W(\sigma)$, i.e.,

$$\langle\Omega\rangle \approx \frac{\frac{1}{N}\sum_n\Phi(\sigma_n)\langle\Omega\rangle_{\sigma_n}}{\frac{1}{N}\sum_n\Phi(\sigma_n)}. \quad (11)$$

Success of the outlined method hinges on the sign $\Phi(\sigma)$ of the weight function $W(\sigma)$. Unfortunately, in the most general case, $\mathrm{Tr}_N U_\sigma(\beta,0)$ is not always positive hence $\Phi(\sigma)$ can be ±1. Such fluctuations causes significant cancellations in the denominator of equation (11) and renders the method ineffective due to large statistical uncertainties in $\langle\Omega\rangle$. In the literature, this problem is referred to as the Monte Carlo sign problem and it is common to Quantum Monte Carlo methods in fermionic many-body problems (see f.x. the review in Ref. [42]). For any Hamiltonian (Eq. (3)) with all $V_\alpha < 0$, h_σ are always time-reversal invariant, since all s_α are real (Eq. (9)). As was shown by Lang et al. [9], time-reversal invariance of h_σ implies that the eigenvalues of the matrix U_σ come in complex-conjugate pairs which, in turn, ensures that the grand-canonical partition function $\mathrm{Tr}U_\sigma$ is positive definite. In the canonical ensemble, projections on even number of particles always preserve the good sign as long as the grand canonical partition function is positive definite. However for systems with odd-number of particles, projections onto an odd number of particles usually reintroduces the sign problem at large values of β even when the grand canonical partition function is positive definite.

Although Quantum Monte Carlo simulations are susceptible to the sign problem for a general two-body interaction and require practical approaches to avoid it [14,36,38,43–50], purely attractive two-body interactions are known to be free of this restriction [36,39]. For the benefit of both nuclear and atomic physics communities, we also demonstrate the absence of the sign problem explicitly for an attractive zero-range interaction in the next section.

4 Sign properties of the zero-range interaction

We now consider the zero-range interaction in the jj-coupling scheme which is discussed in full detail in Appendix A. We write the two-body Hamiltonian in the so-called *pairing* (or *particle-particle*) *decomposition* [9,11] as:

$$H_2 = \frac{1}{2}\sum_{abcd}\sum_{JM}V_J(ab,cd)A^\dagger_{JM}(ab)A_{JM}(cd), \quad (12)$$

where the pair operators are defined by:

$$A^{\dagger}_{JM}(ab) = \sum_{m_a m_b} \langle j_a m_a j_b m_b | JM \rangle a^{\dagger}_{j_b m_b} a^{\dagger}_{j_a m_a}. \quad (13)$$

We now introduce the combined indices $i = (ab)$ and $j = (cd)$ to write $V_J(i,j)$ which is a symmetric matrix. Our goal is to diagonalize the matrix and inspect the signs of the eigenvalues. As demonstrated in reference [9], the interaction will produce no sign problem when all of its eigenvalues are negative. Obviously the problem splits into blocks of given J, so we work in a fixed J subspace.

The crucial observation is that $V_J(ab,cd)$ can be factorized in the following way. Firstly, we define the following quantity:

$$f_J(ab) \equiv \frac{1}{\sqrt{2}}(-1)^{l_a+j_b+1/2}[l_a][l_b][j_a][j_b] \begin{Bmatrix} l_a & j_a & \frac{1}{2} \\ j_b & l_b & J \end{Bmatrix} \times \begin{pmatrix} l_a & l_b & J \\ 0 & 0 & 0 \end{pmatrix} e^{i\theta} \sqrt{\frac{|V_0|}{4\pi}} r R_{n_a l_a}(r) R_{n_b l_b}(r), \quad (14)$$

where $e^{2i\theta} = \mathrm{sgn}(V_0)$ and $[j] = \sqrt{2j+1}$. Notice that $f_J(ab)e^{-i\theta}$ is a purely real number. In terms of the combined indices we now have

$$V_J(i,j) = \int_0^{\infty} dr f_J(i) f_J(j). \quad (15)$$

Since this matrix is real symmetric, there is a basis of orthonormal eigenvectors. Let us denote this basis u^k and the corresponding eigenvalues λ^k. The dimension is given by the number of pairs in the given model space that can couple to total angular momentum J. Consider now for a given k the product $(u^k)^T V_J u^k$, where T denotes the transpose. Inserting the explicit form of V_J we have

$$u^T V_J u = \sum_{ij} u^k(i) V_J(i,j) u^k(j) = \int_0^{\infty} dr \left[\sum_i f_J(i) u^k(i) \right]^2 = \lambda^k, \quad (16)$$

where the last equality follows from the eigenvalue equation and the fact that u^k is normalized. We thus see that the eigenvalues are equal to some real number squared times a phase $e^{2i\theta} = sgn(V_0)$. Therefore, the sign of V_0 is also the sign of the eigenvalues. We thus have the result that any attractive zero-range interaction ($V_0 < 0$) will have no sign problem, whereas the repulsive ($V_0 > 0$) case can never give a positive-definite path integral.

The simple form of $V_J(i,j)$ allows us to prove some further properties of its spectrum. Define (for fixed J not shown) the row vector $f = [f_1 f_2 \dots f_n]$, where n counts the pairs, such as to fulfill $V_J = \int dr f^T f$. Now pick a row vector orthogonal to f so that $fg^T = 0$. Then we see that $V_J g^T = \int dr f^T f g^T = \int dr f^T (f g^T) = 0$, thus all vectors orthogonal to f are in the null-space of V_J. We therefore have only one non-zero eigenvalue for each J and $n-1$ eigenvectors with zero eigenvalue. The sole non-zero eigenvalue has the value $\int dr f f^T$ and the eigenvector f^T. We thus see that the zero-range pairing interaction has a very simple structure after diagonalization.

As mentioned, the above proof was carried out in the so-called pairing decomposition with the operators $A^{\dagger}_{JM}(ab)$ and $A_{JM}(cd)$. In many nuclear applications of the methods, the calculations are carried out in the density decomposition [11]. However, the exact path integral is independent of the particular representation and the above result will still hold. In particular, the change from pairing to density decomposition is in practice a re-coupling of the angular momenta involved (and a change of the one-body terms that we are not concerned with). Since re-couplings corresponds to changes of basis the result for the eigenvalues still holds. In Appendix B, we include a proof based on the m-scheme and the density decomposition for completeness. We have also done explicit numerical checks of this fact and confirmed the general statement.

The good sign properties of the zero-range pairing rested on the fact that it could be factorized, which is more commonly referred to as separability of the zero-range interaction. A non-zero range interaction would not have this property and positive eigenvalues with associated sign problems can be expected. We note again that even with an interaction that has good sign properties, a system with an odd number of particles will still have a sign problem at low temperature [11].

5 Pairing correlations in SMMC

To illustrate the above discussion, we now turn to an example of small Fermi systems and their pairing properties. The lack of sign problems for the zero-range interaction means that the SMMC can be applied. This was done recently and the energetics and convergence properties have been reported in reference [32]. Here we will focus on pairing properties which is another expectation value that is accessible through the SMMC method. The discussion above in fact implies that the two-component Fermi system in a trap can be mapped onto what is known a pure pairing problem due to the simple form of the interaction. Note that the strength of the two-body matrix is state-dependent. This is an important difference in comparison to typical models for large-scale two-component systems that are employed for instance in the BCS theory of conventional macroscopic superconductors.

In the basic Hamiltonian in equation (1), we parametrize the interaction by V_0 which has units of energy times volume. As discussed in reference [32], the interaction strength can be written $V_0 = -g\hbar\omega b^3$ (remember that we consider $V_0 < 0$ only to avoid sign issues), where g is now a convenient dimensionless strength parameter. In experiments on atomic gases the interactions are usually parametrized via the two-body scattering length, a, which can be tuned by applied fields [1]. Relating the value of g to the value of a is therefore crucial and will in general depend on the model space used. Here we will consider g to be a parametric quantity to describe pairing, but for the sake of completeness we note that the values used below, $g = 10$ and $g = 20$ – in a model space consisting of the

major shells of $s+p+sd$ – correspond to $a/b=-1.0$ and $a/b=11$, respectively.

To develop a better understanding for the energetics of the pairing strength considered in this section, we can consider a simple pairing model with the structure

$$H=\sum_i Ga_i^\dagger a_i+\frac{V}{2}\sum_{i,j}a_i^\dagger a_{\bar{i}}^\dagger a_{\bar{j}}a_j, \tag{17}$$

where i,j denotes single-particle levels and $\bar{i}$ is a time-reversed state. G and V are the level spacing and pairing strength, respectively. In units of $G=1$, $V\sim 1$ is a regime of competition between single-particle excitations and pairing, while the regime of $V\sim 10$ is pairing dominated. The model we study here differs from the simple pairing model by having state-dependent matrix elements given by the overlap of different oscillator single-particle states. However; we can still give an overall estimate of the typical matrix elements in units of the single-particle level spacing, $\hbar\omega$. In the regime characterized by $g=10$, magnitude of a typical matrix element is of the order 1 and in the light of the simple model mentioned above, we expect pairing and level structure to be in competition. In comparison, the regime described by $g=20$ should naturally be pairing dominated. These ascertainments are perfectly consistent with the typical discussion of BCS-BEC crossover [1,2] when considering the corresponding values of a/b cited above. Thus, we expect $a/b<0$ and $a/b>0$ to be in the weak and strong pairing regimes, respectively.

To study the pairing properties, we consider the expectation value of a number-conserving BCS-like pair matrix

$$M_{\alpha,\alpha'}=\langle\Delta^\dagger(j_a,j_b)\Delta(j_c,j_d)\rangle, \tag{18}$$

with the $J=0$ pair operator

$$\Delta^\dagger=\frac{1}{\sqrt{1+\delta_{ab}}}\left[a_{j_a}^\dagger\times a_{j_b}^\dagger\right]^{JM=00} \tag{19}$$

where $a_{j_a}^\dagger$ creates a particle in orbit j_a (which is the combination of orbital and spin angular momentum of the fermions). This operator is thus a measure of the pairing content corresponding to $J=0$. An indication of the pairing correlations can be obtained from the sum over all matrix elements, defining the pairing strength in the following [51]. Since we employ a finite temperature formulation of the SMMC method, we, however, need to eliminate the thermal correlations that would be present in the non-interacting system. We therefore subtract the 'mean-field' values – calculated at the same T but with $g=0$ – to obtain the genuine pairing correlations.

The pairing correlations are important in nuclear physics in several respects. A particular example is the influence of pairing on nuclear level density distributions [51] which are crucial for addressing nuclear reactions of astrophysical interest [52]. In cold atomic gases, pairing correlations are observable in what is usually called noise correlations [53]. These two-point correlations have been measured in experiments using optical lattice potentials and are employed to demonstrate bunching for bosonic [54] and anti-bunching for fermionic atoms [55]. The pairing correlations we consider here should therefore be directly measurable in the cold atomic gases. Alternatively, a projection method can be used, wherein one rapidly changes the interaction strength to convert all pairs into molecules [56–61]. The momentum distribution of the molecules can subsequently be measured by turning the trapping potential off, and this carries the imprint of the original many-body state in the trap prior to molecular conversion and release of the system.

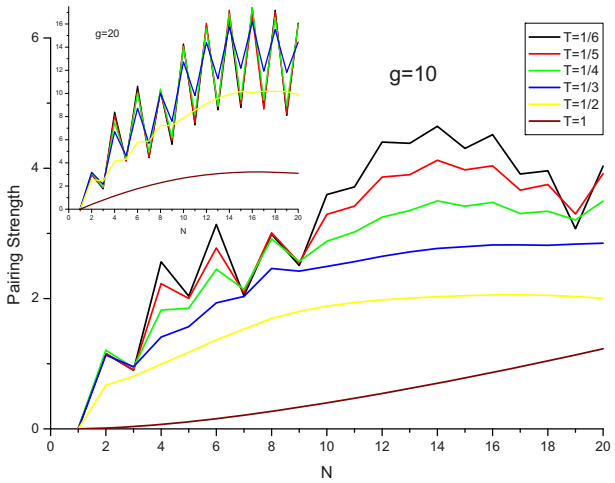

Fig. 1. The pairing strength as a function of particle number, N, for various temperatures, T (in units of $\hbar\omega$) for $g=10$. The upper left inset shows the results for $g=20$. The uncertainties are very small and not shown.

In Figure 1 we show the pairing strength as a function of particle number for different temperatures. The most striking feature is naturally the odd-even staggering. The relative reduction of pairing strength for odd-particle numbers is related to the blocking of scattering of pairs into the orbital occupied by the unpaired particle. The non-interacting systems have closed-shell configurations for $N=2,8,20$. With interaction switched on, these configurations manifest themselves by a relative reduction of the pairing strength (overlaid by a general increase due to a growing number of pairs) and a larger resistance against temperature increase. The strong dips observed for particle numbers $N=7$, 9, and 19 are also connected to the shell closures. Relatedly, the pairing strength is largest for mid-shell systems. In the inset one can see that the staggering is larger for $g=20$ and persists to larger temperatures as expected.

To investigate further the transition between a paired state and a normal state, we show the pairing strength for $g=10$ and $g=20$ as a function of T for selected particle numbers in Figure 2. We note that, in the high temperature regime, pairing correlations are ordered with increasing number of particles (an indication of the equipartitioning in the model space) and that they go through a rapid and monotonous decay. In contrast, the low temperature regime is dominated by structure and odd-even effects. Notice the persistence in the pairing strength in the systems with $N=2$ and $N=8$ (also the case for

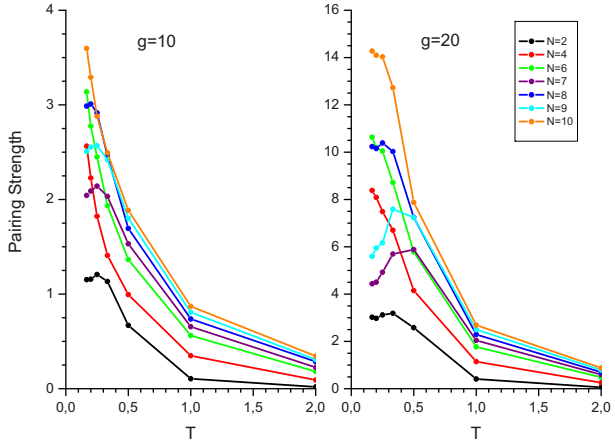

Fig. 2. The pairing strength as a function of temperature, T (in units of $\hbar\omega$), for various particle numbers, N and for $g = 10$ (left) and $g = 20$ (right). Uncertainties are small and not shown. Note the different scales in the two panels.

$N = 20$, which is not shown) due to the shell closures. Shown are also the cases of $N = 7$ and $N = 9$, which exhibit large dips in the pairing strength in Figure 1. They are generally below the neighboring even-N systems at low T, yet again confirming that an unpaired particle has a significant blocking effect on the pairing strength. Furthermore, they have the same structure as the neighboring closed shell $N = 8$, but at lower magnitudes. It is also interesting to observe that, for systems with $N = 7$ and 9, the pairing strength is largest at finite T, reflecting the competition between blocking by the unpaired particle and thermal excitations which moves the unpaired particle across the shell closure reducing the blocking effect. A similar effect has been found in the SMMC studies for nuclei with odd-nucleon numbers [62]. Comparing the $g = 10$ and $g = 20$ results, we see that the above effects are more pronounced for the stronger pairing strength and persists to higher temperature. This is consistent with the discussions above. Similar evidence for a transition at finite T in a homogeneous system in both energy and pair correlation was found in reference [63].

5.1 Connection to other pairing phenomena

Many pairing studies consider only pairs of particles in time-reversed states with an attractive zero-range interaction of constant magnitude $g < 0$. This is, for instance, the case in condensed-matter physics when appyling the simplest version of the BCS pairing theory to a homogeneous Fermi gas with an attractive interaction in relative momentum zero and spin singlet states ($\boldsymbol{k}, \uparrow$ pairs with $-\boldsymbol{k}, \downarrow$ only). This philosophy of pairing time-reversed states can be continued to non-homogeneous systems but at the price of getting a state-dependent gap function, Δ_i, in general, where i denotes the mean-field single-particle levels that are subjected to a pairing interaction. (The mean-field could arise from a Hartree-Fock calculation.).

In nuclear physics, pairing models often employ this restriction, as in the case of the pairing force problem (see Ref. [64]) which has the property that it is exactly solvable. A justification for these models comes from the fact that the pairing force usually has a short-range and for two nucleons in a single mean-field level, the total $J = 0$ pairs have the strongest gain in binding [64]. In this single level case, these pairs are built from time-reversed states [65].

If we consider the case of cold atomic gases, we start from the zero-range interaction and an external trap providing the mean-field. In a BCS picture, this implies that we have general matrix elements (as given in Eq. (A.6)) and a state-dependent gap, Δ_i. However, there are now different regimes of interest depending on the strength, g, and the level spacing, $\hbar\omega$. This has been discussed in references [66,67] using the Bogoliubov-de Gennes equations (more commonly called the Hartree-Fock-Bogoliubov equations in nuclear physics) along with the local density approximation to describe larger systems. There it was found that an intra- and an inter-shell pairing regime appears, depending on whether the typical gap parameter satisfies $\Delta < \hbar\omega$ (intra) or $\Delta > \hbar\omega$ (inter). Since the zero-range interactions which are employed in the Bogoliubov-de Gennes approach are precisely time-reversed, one has $l_a = l_b$ and $l_c = l_d$ in equation (A.6).

Here we are concerned with small systems, and it is clear that the mean-field Bogoliubov-de Gennes should break down as particle numbers become small, and correlations beyond the mean-field are strong. In order to get a quantitative feeling for these additional correlations we can compare a model where only time-reversed states are used in the interaction ($l_a = l_b$ and $l_c = l_d$) and the full zero-range interaction where all states that give non-zero contributions to equation (A.6) are taken into account. It can be readily observed that our proof of good sign properties will hold in both cases (time-reversed states are a special case) and the SMMC should work perfectly well.

In Figure 3, we plot the energy of systems with particle numbers of $N = 1$–20 for two kinds of interaction; one that pairs only the time-reversed states (dashed line) and the full zero-range interaction (solid line) in both the weak ($g = 10$ in the upper panel) and the strong pairing ($g = 20$ in the lower panel) regimes. In general, we see that the full interaction gives a somewhat higher energy than the time-reversed one. This is most likely caused by the fact that the full interaction allows low-lying pairs to correlate with pairs in higher shells and thus raise the energy. We see that both interactions capture the shell effect at $N = 8$, while the full interaction seems to produce more structured odd-even effects due to strong pairing. In the overall, however, we do not observe a pronounced difference between a pairing interaction involving only time-reversed states and the full zero-range pairing interaction, the latter being the physical interaction employed in studies of ultracold atomic Fermi gases. Our findings thus indicate that pairing involving only time-reserved states can be a good approximation for the study of small systems as well. Of course, we have to stress that in this limit the shell structure effects are very important and we do not expect this to be captured accurately by local-density

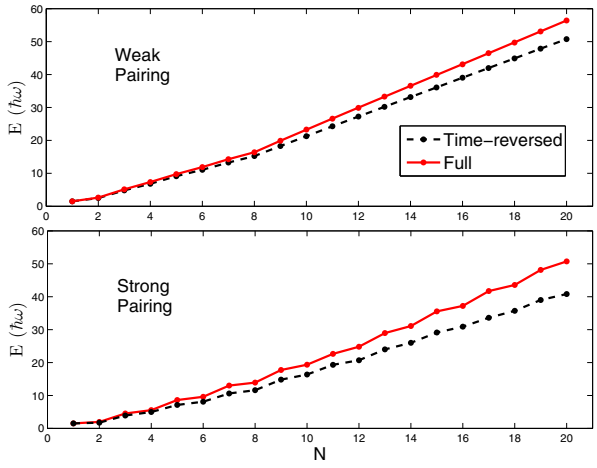

Fig. 3. The energy in units of $\hbar\omega$ of as function of particle number N for time-reversed only (dashed line) and full (solid line) interaction as discussed in the text. Upper panel is for strength $g = 10$ (weak pairing), while the lower one has $g = 20$ (strong pairing).

approximations; thus, the full discrete external trap spectrum must be considered.

6 Summary and outlook

Studies of small two-component Fermi systems in tight external traps are currently being pursued experimentally [4,5] in the realm of cold atomic gas physics. Here we demonstrate how the mapping of the atomic system to an equivalent problem in nuclear physics can be achieved. It has the important feature that there is no sign problem associated with the typical choice of a zero-range interaction within the grand-canonical formulation of the SMMC approach. As we have discussed, the atomic interaction between the two internal hyperfine states is more general than the typical pairing force used in many investigations, and it was therefore not a priori clear that the corresponding nuclear SMMC problem would be free of the sign problem. The alternative approach of using large-scale shell-model diagonalization however, is computationally challenged by the number of configurations which grows exponentially with the model space size; in contrast, the size of the problem scales only quadratically in the SMMC approach [11]. Truncation of the model space may be used to reduce the size of the problem to a certain extent. In low-dimensional systems, which are currently under intense study in atomic physics, the reduced size of the matrix problem may allow a direct diagonalization of the many-body Hamiltonian (a recent pairing study using nuclear-inspired methods can be found in Ref. [68]). However, in the full three-dimensional case, the SMMC method seems to be the only tractable approach at the moment.

We note that there is growing interest in multi-component Fermi systems in atomic gas physics. Three-component mixtures of ^{6}Li have been realized a few years ago and continue to be a hot topic [69–74]. Fermionic systems with four or more components are also being pursued since it is possible to realize such systems by using not alkali but rather alkali-earth atoms which can have many degenerate hyperfine states, allowing the realization of many interesting models of magnetism and pairing [75–77]. From a nuclear physics point-of-view, a multi-component system can be mapped onto the isospin degree of freedom. In the case of four-component Fermi systems, one should therefore be able to perfectly map the problem onto the isospin 1/2 times spin 1/2 formalism and exploit the corresponding advanced calculational tools available in nuclear physics.

In closing, we would also like to point out that spin-orbit coupling has recently become a heavily pursued topic in ultracold atomic systems since it is now possible to implement by optical means for both bosonic [78,79] and fermionic atomic systems [80,81]. These studies produce a spin-orbit coupling of the kind used in mostly condensed matter and solid state, which has the form of $\boldsymbol{s} \cdot \boldsymbol{k}$, i.e. of a spin-linear momentum coupling. However, it was recently shown that it is possible to use applied optical fields that impart orbital angular momentum instead of linear momentum on atoms [82,83]. It should thus be within reach to create terms that are similar to the traditional spin-orbit term encountered in nuclear physics, i.e. of the form of $\boldsymbol{s} \cdot \boldsymbol{l}$. This would immediately imply that the jj-coupling be the more suitable approach for the study of small atomic Fermi systems with optically induced spin-orbit interactions. Since the external laser intensity is typically a multiplicative factor on the coupling terms, we expect that one can correspondingly address the full range of spin-orbit strength from weak to strong, both experimentally and theoretically.

Note added in proof. A related study of small Fermi systems using a method very similar to the one discussed here has been presented in reference [39]. That study considers pairing correlations defined in a similar fashion to our equation (18).

We acknowledge fruitful discussions with Karlheinz Langanke, David Dean, Klaus Mølmer and Christopher Gilbreth. C.Ö. thanks Thomas Pappenbrock for suggestions on the current work. N.T.Z. would like to thank Niels Leth Gammelgaard, Thomas Kragh, and Mark S. Rudner for enlightening discussion on some linear algebraic details, and David Pekker for reading and commenting on an early draft. We thank the referees for comments and suggestions that have improved the presentation and discussion.

Appendix A: The zero-range force in the jj-coupling scheme

To make explicit the rotational invariance in nuclear applications, matrix elements of the two-body interaction are often specified in the jj-coupling scheme by:

$$V_J(ab,cd) = \Big\langle [\psi_{j_a}(\vec{r}_1) \times \psi_{j_b}(\vec{r}_2)]^{JM} | V(\vec{r}_1,\vec{r}_2) | \times [\psi_{j_c}(\vec{r}_1) \times \psi_{j_d}(\vec{r}_2)]^{JM} \Big\rangle, \quad \text{(A.1)}$$

where a, b, c and d denote single-particle orbitals and j_a, j_b, j_c, and j_d are their respective angular momenta. Notice that V_J is independent of the total projection M (as can be seen by applying the Wigner-Eckart theorem). In analogy with the nuclear shell-model, single-particle orbitals associated with an external mean field (here assumued to be spherical) carry the quantum numbers (nlm_l) and the internal (spin-half) quantum numbers $(\frac{1}{2}m_s)$. The external and internal angular momenta can be coupled through $\vec{j} = \vec{l} + \vec{s}$ to give the total angular momentum $j = l \pm 1/2$ for a given single-particle orbital.

As discussed in the main text, the zero-range interaction we employ connects only two-body states with spin-singlet internal states; $|S = 0, M_s = 0\rangle$. To this end, it is more convenient to transform the jj-coupling scheme to the LS-coupling scheme. This can easily be achieved using the standard techniques of angular momentum [65]:

$$|(l_a s_a) j_a, (l_b s_b) j_b, JM\rangle = \sum_{L,S} [L][S][j_a][j_b] \begin{Bmatrix} l_a & s_a & j_a \\ l_b & s_b & j_b \\ L & S & J \end{Bmatrix} \times |(l_a l_b) L, (s_a s_b) S, JM\rangle . \tag{A.2}$$

Here we are interested in the $s_a = s_b = 1/2$ case, and, since the interaction contains a projection onto spin singlet states, only need the $S = 0$ component of this transformation. Using a reduction on the $9j$ symbol [65], the projection can be written

$$P_{S=0}|(l_a \tfrac{1}{2}) j_a, (l_b \tfrac{1}{2}) j_b, JM\rangle = \sum_{L} [L][j_a][j_b] \begin{Bmatrix} l_a & \frac{1}{2} & j_a \\ l_b & \frac{1}{2} & j_b \\ L & 0 & J \end{Bmatrix} \times |(l_a l_b) L, \left(\frac{1}{2}\frac{1}{2}\right) 0, JM\rangle = (-1)^{L+l_a+j_b+2j_a-1/2} \times \frac{[j_a][j_b]}{\sqrt{2}} \begin{Bmatrix} L & j_a & j_b \\ 1/2 & l_b & l_a \end{Bmatrix} \delta_{LJ} |(l_a l_b) L, \left(\frac{1}{2}\frac{1}{2}\right) 0, JM\rangle, \tag{A.3}$$

where $P_{S=0} = (1 - \boldsymbol{\sigma}_1 \cdot \boldsymbol{\sigma}_2)/4$ is the projection onto the spin singlet state. The remaining zero-range interaction of course only acts on the external quantum states, thus we have to evaluate matrix elements between coupled states with operators acting on only one of the degree of freedom. Since the spin part is trivial for singlets we simply have the result (keeping both L and J for clarity even though $L = J$)

$$\left\langle (l_a l_b) L, \left(\frac{1}{2}\frac{1}{2}\right) 0, JM \left| V(\vec{r}_1 - \vec{r}_2) \right| (l_c l_d) L, \left(\frac{1}{2}\frac{1}{2}\right) 0, JM \right\rangle = \langle (l_a l_b) LM \left| V(\vec{r}_1 - \vec{r}_2) \right| (l_c l_d) LM \rangle , \tag{A.4}$$

where we have explicitly indicated the orbital angular momenta of all states involved. For the zero-range interaction $V(\vec{r}_1 - \vec{r}_2) = V_0 \delta(\vec{r}_1 - \vec{r}_2)$, the latter matrix element can be found in many textbooks (see for instance [65]) and is given by:

$$\langle l_1 l_2 JM | V_0 \delta(\vec{r}_1 - \vec{r}_2) | l_1' l_2' J' M' \rangle = \delta_{J,J'} \delta_{M,M'} [l_1][l_2][l_1'][l_2'] \times \begin{pmatrix} l_1 & l_2 & J \\ 0 & 0 & 0 \end{pmatrix} \begin{pmatrix} l_1' & l_2' & J \\ 0 & 0 & 0 \end{pmatrix} \times \frac{V_0}{4\pi} \int_0^\infty dr r^2 R_{n_1 l_1}(r) R_{n_2 l_2}(r) R_{n_1' l_1'}(r) R_{n_2' l_2'}(r). \tag{A.5}$$

We can now insert all these formulae into equation (A.1) to get an expression for the J-scheme interaction:

$$\begin{aligned} V_J(ab, cd) &= \delta_{J,L} (-1)^{l_a+l_c+2j_a+2j_c+j_b+j_d-1} \frac{[j_a][j_b][j_c][j_d]}{2} \\ &\quad \times \begin{Bmatrix} L & j_a & j_b \\ \frac{1}{2} & l_b & l_a \end{Bmatrix} \begin{Bmatrix} L & j_c & j_d \\ \frac{1}{2} & l_d & l_c \end{Bmatrix} \\ &\quad \times \langle (l_a l_b) L0 | V(\vec{r}_1 - \vec{r}_2) | (l_c l_d) L0 \rangle \\ &= (-1)^{j_b+j_d+l_a+l_c+1} \frac{[j_a][j_b][j_c][j_d]}{2} \\ &\quad \times \begin{Bmatrix} J & j_a & j_b \\ \frac{1}{2} & l_b & l_a \end{Bmatrix} \begin{Bmatrix} J & j_c & j_d \\ \frac{1}{2} & l_d & l_c \end{Bmatrix} \\ &\quad \times [l_a][l_b][l_c][l_d] \begin{pmatrix} l_a & l_b & J \\ 0 & 0 & 0 \end{pmatrix} \begin{pmatrix} l_c & l_d & J \\ 0 & 0 & 0 \end{pmatrix} \frac{V_0}{4\pi} \\ &\quad \times \int_0^\infty dr r^2 R_{n_a l_a}(r) R_{n_b l_b}(r) R_{n_c l_c}(r) R_{n_d l_d}(r), \end{aligned} \tag{A.6}$$

where the second equality comes from using the formula in equation (A.5). Notice that the phase can be written with $l_b + l_d$ instead of $l_a + l_c$ since $l_a + l_b + l_c + l_d$ is even due to the restrictions from the Clebsch-Gordon coefficients. This is the general interaction in the spin singlet state and l_a, l_b, l_c, and l_d can in general be different as long as they couple pairwise to $L = J$. For the pairing interaction in the time-reversed states discussed in the text, we have $l_a = l_b$ and $l_c = l_d$.

The formula above explicitly shows that $l_a + l_b + J$ and $l_c + l_d + J$ must be even. However, the multipole expansion used to arrive at this expression implicitly requires that also $l_a + l_c + J$ and $l_b + l_d + J$ be even. Notice also that the factor $l_a + l_c$ means that pairing across two opposite parity major shells can be repulsive for $V_0 < 0$. This is well-known in nuclear pairing studies [11].

As discussed in reference [11], the physical matrix elements used in the nuclear shell-model must be antisymmetrized. This can be achieved by using the definition

$$V_J^A(ab, cd) = \frac{1}{\sqrt{(1 + \delta_{ab})(1 + \delta_{cd})}} \times \left[V_J(ab, cd) - (-1)^{j_c+j_d-J} V_J(ab, dc) \right] . \tag{A.7}$$

However, as by angular momentum algebra one may show that $V_J(ab, dc) = -(-1)^{j_c+j_d-J} V_J(ab, cd)$. Thus we have the simple result

$$V_J^A(ab, cd) = \frac{2}{\sqrt{(1 + \delta_{ab})(1 + \delta_{cd})}} V_J(ab, cd). \tag{A.8}$$

This is not surprising since we argued that only the antisymmetric $S = 0$ spin-singlet component should have non-zero matrix elements. We have effectively enforced the Pauli principle in this manner.

Appendix B: Sign properties in the m-scheme

It is also possible to demonstrate that the contact interaction is free of the sign problem in the so-called *density decomposition* [11]. For convenience, we define the single-particle states by $|nlms\sigma\rangle \equiv |am\sigma\rangle$ where $a = (nl)$ and $\sigma = \pm 1/2$. In the m-scheme approach, the two-body part of the Hamiltonian (we omit the one-body term without loss of generality) can be written as:

$$H_2 = \frac{1}{2} \sum_{\substack{abcd \\ mm'\sigma\sigma'}} V_{abcd} a^\dagger_{am\sigma} a^\dagger_{bm'\sigma'} a_{dm'\sigma'} a_{cm\sigma} \tag{B.1}$$

where we used the spin-independence of the interaction explicitly. Also notice that the contact interaction should not change the m-quantum number of the orbital angular momentum states, hence V_α are labelled by only the nl-quantum numbers of the states. H_2 can be brought into the density decomposition by a rearrangement of the creation and annihilation operators. The new two-body Hamiltonian (up to an additional one-body term), is now written as:

$$\begin{aligned} H_2' &= \frac{1}{2} \sum_{\substack{abcd \\ mm'\sigma\sigma'}} V_{abcd} a^\dagger_{am\sigma} a_{cm\sigma} a^\dagger_{bm'\sigma'} a_{dm'\sigma'} \\ &= \frac{1}{2} \sum_{ij} V_{ij} \rho_i \rho_j \end{aligned} \tag{B.2}$$

where $i = (ac)$ indicate two-body (particle-hole) indices and $\rho_i = \sum_{m\sigma} a^\dagger_{am\sigma} a_{cm\sigma}$ are density operators. Since V_{ij} is a real symmetric matrix, it can be diagonalized by an orthogonal transformation

$$V_{ij} = \sum_\alpha \lambda_\alpha O_{\alpha i} O_{\alpha j}. \tag{B.3}$$

Using this expression, H_2' can be brought into a quadratic form:

$$H_2' = \frac{1}{2} \sum \lambda_\alpha P_\alpha^2 \tag{B.4}$$

where $P_\alpha = \sum_\alpha O_{\alpha i} \rho_i$. To manifest the time-reversal properties, we now express H_2' in a similar form to the two-body term in equation (3). To this end, we introduce the time-reversed creation and annihilation operators in the Condon-Shortley phase convention (where the state $|lm\rangle$ is defined in terms of the spherical harmonics without the i^l factor):

$$\begin{aligned} \bar{a}^\dagger_{nlm\sigma} &= (-1)^l (-1)^{l+m+1/2+\sigma} a^\dagger_{nl-m-\sigma} \\ &= (-1)^{m+1/2+\sigma} a^\dagger_{nl-m-\sigma} \end{aligned} \tag{B.5}$$

$$\begin{aligned} \bar{a}_{nlm\sigma} &= (-1)^l (-1)^{l+m+1/2+\sigma} a_{nl-m-\sigma} \\ &= (-1)^{m+1/2+\sigma} a_{nl-m-\sigma}. \end{aligned} \tag{B.6}$$

Using these, we obtain

$$\begin{aligned} \bar{\rho}_i &= \sum_{m\sigma} \bar{a}^\dagger_{am\sigma} \bar{a}_{cm\sigma} \\ &= \sum_{m\sigma} (-1)^{2(m+1/2+\sigma)} a^\dagger_{a-m-\sigma} a_{c-m-\sigma} = \rho_i, \end{aligned} \tag{B.7}$$

from which it follows that $\bar{P}_\alpha = P_\alpha$. Hence we can write

$$H_2' = \frac{1}{4} \sum_\alpha \lambda_\alpha \left\{ P_\alpha, \bar{P}_\alpha \right\}. \tag{B.8}$$

The condition for a good-sign interaction, that h_σ (Eq. (9)) is time-reversally invariant, demands that all $\lambda_\alpha < 0$. For the contact interaction, $v = -g\delta(\mathbf{r} - \mathbf{r}')$, the matrix V_{ij} is negative-definite since

$$V_{ij} = V_{abcd} \sim -g \int dr r^2 R^2_{nl}(r) R^2_{n'l'}(r) < 0, \tag{B.9}$$

thus the good-sign property is established.

References

1. I. Bloch, J. Dalibard, W. Zwerger, Rev. Mod. Phys. **80**, 885 (2008)
2. S. Giorgini, L.P. Pitaevskii, S. Stringari, Rev. Mod. Phys. **80**, 1215 (2008)
3. W. Ketterle, M.W. Zwierlein, in *Proceedings of the International School of Physics "Enrico Fermi", Varenna, 2006*, edited by M. Inguscio, W. Ketterle, C. Salomon (IOS Press, Amsterdam, 2008), Course CLXIV
4. F. Serwane, G. Zürn, T. Lompe, T.B. Ottenstein, A.N. Wenz, S. Jochim, Science **332**, 6027 (2011)
5. G. Zürn, F. Serwane, T. Lompe, A.N. Wenz, M.G. Ries, J.E. Bohn, S. Jochim, Phys. Rev. Lett. **108**, 075303 (2012)
6. A. Bohr, B.R. Mottelson, D. Pines, Phys. Rev. **110**, 936 (1958)
7. J. Carlson, S. Gandolfi, A. Gezerlis, Prog. Theor. Exp. Phys. **2012**, 01A209 (2012)
8. N.T. Zinner, A.S. Jensen, J. Phys. G **40**, 053101 (2013)
9. G.H. Lang, C.W. Johnson, S.E. Koonin, W.E. Ormand, Phys. Rev. C **48**, 1518 (1993)
10. Y. Alhassid, D.J. Dean, S.E. Koonin, G. Lang, W.E. Ormand, Phys. Rev. Lett. **72**, 613 (1994)
11. S.E. Koonin, D.J. Dean, K. Langanke, Phys. Rep. **278**, 1 (1997)
12. S.Y. Chang, G.F. Bertsch, Phys. Rev. A **76**, 021603(R) (2007)
13. D. Blume, J. von Stecher, C.H. Greene, Phys. Rev. Lett. **99**, 233201 (2007)
14. M.M. Forbes, S. Gandolfi, A. Gezerlis, Phys. Rev. A **86**, 053603 (2012)
15. D. Blume, Rep. Prog. Phys. **75**, 046401 (2012) and references therein
16. T. Busch, B.G. Englert, K. Rzążewski, M. Wilkens, Found. Phys. **28**, 548 (1998)
17. T. Stöferle, H. Moritz, K. Günter, M. Köhl, T. Esslinger, Phys. Rev. Lett. **96**, 030401 (2006)
18. T. Volz et al., Nat. Phys. **2**, 692 (2006)

19. G. Thalhammer et al., Phys. Rev. Lett. **96**, 050402 (2006)
20. C. Ospelkaus et al., Phys. Rev. Lett. **97**, 120402 (2006)
21. W.C. Haxton, T. Luu, Phys. Rev. Lett. **89**, 182503 (2002)
22. I. Stetcu, B.R. Barrett, U. van Kolck, Phys. Lett. B **653**, 358 (2007)
23. I. Stetcu, B.R. Barrett, U. van Kolck, J.P. Vary, Phys. Rev. A **76**, 063613 (2007)
24. Y. Alhassid, G.F. Bertsch, L. Fang, Phys. Rev. Lett. **100**, 230401 (2008)
25. I. Stetcu, J. Rotureau, B.R. Barrett, U. van Kolck, Ann. Phys. **325**, 1644 (2010)
26. T. Luu, M.J. Savage, A. Schwenk, J.P. Vary, Phys. Rev. C **82**, 034003 (2010)
27. J. Rotureau, I. Stetcu, B.R. Barrett, M.C. Birse, U. van Kolck, Phys. Rev. A **82**, 032711 (2010)
28. J.R. Armstrong, N.T. Zinner, D.V. Fedorov, A.S. Jensen, J. Phys. B **44**, 055303 (2011)
29. S. Tölle, H.-W. Hammer, B.C. Metsch, C. R. Phys. **12**, 59 (2011)
30. C.N. Gilbreth, Y. Alhassid, Phys. Rev. A **85**, 033621 (2012)
31. J.R. Armstrong, N.T. Zinner, D.V. Fedorov, A.S. Jensen, Phys. Rev. E **85**, 021117 (2012)
32. N.T. Zinner, K. Mølmer, C. Özen, D.J. Dean, K. Langanke, Phys. Rev. A **80**, 013613 (2009)
33. S. Zhang, J. Carlson, J.E. Gubernatis, Phys. Rev. Lett. **74**, 3652 (1995)
34. S. Zhang, J. Carlson, J.E. Gubernatis, Phys. Rev. B **55** 7464 (1997)
35. S. Zhang, H. Krakauer, Phys. Rev. Lett. **90**, 136401 (2003)
36. A. Bulgac, J.E. Drut, P. Magierski, Phys. Rev. Lett. **96**, 090404 (2006)
37. D. Lee, Phys. Rev. B **73**, 115112 (2006)
38. A. Mukherjee, Y. Alhassid, Phys. Rev. A **88**, 053622 (2013)
39. C. Gilbreth, Y. Alhassid, Phys. Rev. A **88**, 063643 (2013)
40. J. Hubbard, Phys. Rev. Lett. **3**, 77 (1959)
41. R.L. Stratonovich, Dokl. Akad. Nauk. S.S.S.R. **115**, 1097 (1957)
42. W. von der Linden, Phys. Rep. **220**, 53 (1992)
43. D.J. Scalapino, R.L. Sugar, Phys. Rev. Lett. **46**, 519 (1981)
44. J.-W. Chen, D.B. Kaplan, Phys. Rev. Lett. **92**, 257002 (2004)
45. J. Carlson, S.Y. Chang, V.R. Pandharipande, K.E. Schmidt, Phys. Rev. Lett. **91**, 050401 (2003)
46. G.E. Astrakharchik, J. Boronat, J. Casulleras, S. Giorgini, Phys. Rev. Lett. **93**, 200404 (2004)
47. E. Burovski, N. Prokofev, B. Svistunov, M. Troyer, New J. Phys. **8**, 153 (2006)
48. P. Magierski, G. Wlazlowski, A. Bulgac, J.E. Drut, Phys. Rev. Lett. **103**, 210403 (2009)
49. M.G. Endres, D.B. Kaplan, J.-W. Lee, A.N. Nicholson, Phys. Rev. A **84**, 043644 (2011)
50. J. Carlson, S. Gandolfi, K.E. Schmidt, S. Zhang, Phys. Rev. A **84**, 061602(R) (2011)
51. C. Özen, K. Langanke, G. Martínez-Pinedo, D.J. Dean, Phys. Rev. C **75**, 064307 (2007)
52. T. Rauscher, F.-K. Thielemann, K.-L. Kratz, Phys. Rev. C **56**, 1613 (1997)
53. E. Altman, E. Demler, M.D. Lukin, Phys. Rev. A **70**, 013603 (2004)
54. S. Fölling et al., Nature **434**, 481 (2005)
55. T. Rom et al., Nature **444**, 733 (2006)
56. M. Greiner, C.A. Regal, D.S. Jin, Nature **426**, 537 (2003)
57. C.A. Regal, M. Greiner, D.S. Jin, Phys. Rev. Lett. **92**, 040403 (2004)
58. M.W. Zwierlein, C.A. Stan, C.H. Schunck, S.M.F. Raupach, A.J. Kerman, W. Ketterle, Phys. Rev. Lett. **92**, 120403 (2004)
59. R.B. Diener, T.L. Ho, `arXiv:cond-mat/0404517`
60. E. Altman, A. Vishwanath, Phys. Rev. Lett. **95**, 110404 (2005)
61. I. Zapata et al., Phys. Rev. Lett. **105**, 095301 (2010)
62. J. Engel, K. Langanke, P. Vogel, Phys. Lett. B **429**, 215 (1998)
63. V.K. Akkineni, D.M. Ceperley, N. Trivedi, Phys. Rev. B **76**, 165116 (2007)
64. A.L. Fetter, J.D. Walecka, *Quantum Theory of Many-Particle Systems* (McGraw-Hill, San Francisco, 1971)
65. D.M. Brink, G.R. Satchler, *Angular Momentum* (Oxford University Press Inc., New York, 1993)
66. H. Heiselberg, B. Mottelson, Phys. Rev. Lett. **88**, 190401 (2002)
67. G.M. Bruun, H. Heiselberg, Phys. Rev. A **65**, 053407 (2002)
68. M. Rontani, J.R. Armstrong, Y. Yu, S. Åberg, S.M. Reimann, Phys. Rev. Lett. **102**, 060401 (2009)
69. S. Nakajima, M. Horikoshi, T. Mukaiyama, P. Naidon, M. Ueda, Phys. Rev. Lett. **106**, 143201 (2011)
70. T. Lompe, T.B. Ottenstein, F. Serwane, A.N. Wenz, G. Zürn, S. Jochim, Science **330**, 940 (2010)
71. J.H. Huckans, J.R. Williams, E.L. Hazlett, R.W. Stites, K.M. O'Hara, Phys. Rev. Lett. **102**, 165302 (2009)
72. J.R. Williams et al., Phys. Rev. Lett. **103**, 130404 (2009)
73. T.B. Ottenstein, T. Lompe, M. Kohnen, A.N. Wenz, S. Jochim, Phys. Rev. Lett. **101**, 203202 (2008)
74. S. Nakajima, M. Horikoshi, T. Mukaiyama, P. Naidon, M. Ueda, Phys. Rev. Lett. **105**, 023201 (2010)
75. H. Hara et al., Phys. Rev. Lett. **106**, 205304 (2011)
76. A.V. Gorshkov et al., Nat. Phys. **6**, 289 (2010)
77. S. Taie et al., Phys. Rev. Lett. **105**, 190401 (2010)
78. Y.-J. Lin, R.L. Compton, K. Jiménez-García, J.V. Porto, I.B. Spielman, Nature **462**, 628 (2009)
79. Y.-J. Lin, K. Jiménez-García, I.B. Spielman, Nature **471**, 83 (2011)
80. P. Wang et al., Phys. Rev. Lett. **109**, 095301 (2012)
81. L.W. Cheuk et al., Phys. Rev. Lett. **109**, 095302 (2012)
82. S. Moulder, S. Beattie, R.P. Smith, N. Tammuz, Z. Hadzibabic, Phys. Rev. A **86**, 013629 (2012)
83. S. Beattie, S. Moulder, R.J. Fletcher, Z. Hadzibabic, Phys. Rev. Lett. **110**, 025301 (2013)